CONDENSED
MATTER
PHYSICS

Ground state properties of the bond alternating spin-$\frac{1}{2}$ anisotropic Heisenberg chain

S. Paul[1], A.K. Ghosh[2]

[1] Department of Physics, Scottish Church College, Urquhart Square, Kolkata 700006, India

[2] Department of Physics, Jadavpur University, 188 Raja Subodh Chandra Mallik Road, Kolkata 700032, India

Ground state properties, dispersion relations and scaling behaviour of spin gap of a bond alternating spin-$\frac{1}{2}$ anisotropic Heisenberg chain have been studied where the exchange interactions on alternate bonds are ferromagnetic (FM) and antiferromagnetic (AFM) in two separate cases. The resulting models separately represent nearest neighbour (NN) AFM-AFM and AFM-FM bond alternating chains. Ground state energy has been estimated analytically by using both bond operator and Jordan-Wigner representations and numerically by using exact diagonalization. Dispersion relations, spin gap and several ground state orders have been obtained. Dimer order and string orders are found to coexist in the ground state. Spin gap is found to develop as soon as the non-uniformity in alternating bond strength is introduced in the AFM-AFM chain which further remains non-zero for the AFM-FM chain. This spin gap along with the string orders attribute to the Haldane phase. The Haldane phase is found to exist in most of the anisotropic region similar to the isotropic point.

Key words: bond alternating, spin gap, bond operator, string orders, dimer order, scaling law

PACS: 75.10.Jm, 75.10.Pq, 75.50.Ee, 75.40.Mg, 75.30.Gw

1. Introduction

The spin-$\frac{1}{2}$ Heisenberg chains with an energy gap (spin gap) just above the ground state attract immense interest since they give rise to many exotic properties in the ground state. The isotropic AFM and FM spin-$\frac{1}{2}$ Heisenberg chains are exactly solvable by using the Bethe-Ansatz technique both in the presence and in the absence of uniform magnetic field in which energy spectrum is gapless below a critical field [1]. On the other hand, according to Haldane's conjecture [2], AFM Heisenberg chain with integer spin values has a finite spin gap between non-magnetic ground state and the lowest excited state which is known as the Haldane gap. The Haldane phase can be characterized by the finite value of string order parameter [3, 4]. The existence of this spin gap can be explained from the incongruousness of this system with the Lieb-Schultz-Mattis (LSM) theorem [5]. According to the modified version of LSM theorem extended by Affleck and Lieb [6], the SU(2) invariant AFM chains with half-integer spins per unit cell either have gapless excitations or degenerate ground states in the thermodynamic limit, $N \to \infty$. Finally, it has been extended to more than one dimension and shown to be valid for short range interactions with global U(1) symmetry and half-integer spin per unit cell [7].

A spin gap in AFM bond alternating spin-$\frac{1}{2}$ Heisenberg chain was first predicted theoretically in 1962 by Bulaevskii [8]. The nature of triplet excitations at finite temperatures [9] and multimagnon excitations [10] in bond alternating chain has been studied. Hidden $Z_2 \times Z_2$ symmetry breaking along with the Haldane phase is found by Kohmoto [11]. Magnetization process in anisotropic bond alternating chain has been investigated by Totsuka [12]. In the bond alternating spin-$\frac{1}{2}$ Heisenberg chains, the full translational symmetry of the lattice is lost since a unit cell contains two lattice sites. These two spin-$\frac{1}{2}$ degrees of freedom combine to form either total spin 0 or 1. This situation does not comply with the

LSM theorem though the system has global U(1) symmetry. From this point of view, a gap in the spin excitation may appear in the bond alternating chain. The existence of Haldane gap is found in an exactly solvable AFM one-dimensional bilinear-biquadratic spin-1 model where the ground state has a valence bond solid structure in which each integer spin value is described as a symmetric combination of two half-integer spins forming a singlet state within each pair of adjacent sites [13, 14]. In 1992, Hida pointed out that isotropic $S = \frac{1}{2}$ Heisenberg chain with alternating AFM and FM couplings can be mapped onto the isotropic $S = 1$ AFM Heisenberg chain when the FM couplings tend to infinity [15]. Therefore, the existence of Haldane phase can be justified in the $S = \frac{1}{2}$ Heisenberg chains with bond alternation. A transition from Haldane phase to gapless phase has been predicted in the presence of magnetic field [16]. A number of compounds are discovered whose properties can be explained by invoking either AFM-AFM or AFM-FM types of bond alternating chains. For examples, the compounds like $CuGeO_3$ [17], tetrathiafulvalene (TTF) with bisdithiolene metal complexes [18], TTFCuBDT [19], MEM-$(TCNQ)_3$ [20] and many others which show spin-Peierls transitions belong to AFM-AFM bond alternating class. On the other hand, zinc-verdazyl complex [21], α-$CuNb_2O_6$ [22, 23], $Na_3Cu_2SbO_6$ [24], $(CH_3)_2CHNH_3CuCl_3$ [25], and $DMACuCl_3$ [26] belongs to the $S = \frac{1}{2}$ AFM-FM bond alternating class.

In this work, anisotropic bond alternating $S = \frac{1}{2}$ Heisenberg chains with alternating AFM-AFM and AFM-FM couplings have been studied separately where the ground state energy, dispersion relations, ground state orders and the magnitude of spin gap have been obtained for the entire range of anisotropic parameters. Two different theoretical approaches, say, bond operator and Jordan-Wigner representations are employed in which the spin model is expressed in terms of bosonic and fermionic operators, respectively. Mean-field analysis on these two approaches gives rise to accurate results of this model in two different regimes. Ground state energy, dispersion relations, dimer order and spin gap are obtained by using the bond operator formalism. All those properties in addition to string orders have been separately estimated by using exact diagonalization method. Coexistence of dimer and string order parameters has been found. The existence of the spin gap along with the string orders found in most of the anisotropic region attributes to the Haldane phase. We should like to report that this observation is similar to that found at the isotropic point of these models as predicted before [15].

The bond alternating spin model is defined by the Hamiltonian

$$H = \sum_{i=1}^{N/2} \left[J_1 \left(S_{2i-1}^x S_{2i}^x + S_{2i-1}^y S_{2i}^y + \Delta S_{2i-1}^z S_{2i}^z \right) + J_2 \left(S_{2i}^x S_{2i+1}^x + S_{2i}^y S_{2i+1}^y + \Delta S_{2i}^z S_{2i+1}^z \right) \right]. \tag{1.1}$$

N is the total number of spins which is even. The model has the global U(1) symmetry since the z-component of the total spin, S_T^z, is a good quantum number. The J_1 bond is always AFM but the J_2 bond is considered both AFM and FM, such that $-1.0 < \frac{J_2}{J_1} < 1.0$. Δ is the anisotropic parameter. For $J_1 = J_2$, the system remains gapless throughout the anisotropic regime $0 \leqslant \Delta \leqslant 1$, while the spin gap opens up when $J_1 \neq J_2$.

Section 2 contains the results obtained for a four-spin bond alternating plaquette. In sections 3 and 4, investigations based on bond operator and Jordan-Wigner representations are described, respectively. The spin model is studied numerically by using Lanczos exact diagonalization technique where ground state energy and spin gap are obtained and reported in section 5. Values of several ground state orders have been estimated and described in section 6. Section 7 contains a discussion of the results obtained.

2. Four-site bond alternating anisotropic Heisenberg plaquette

Before the beginning of an extensive many-particle formalism, let us explain the results of a four-spin ($N = 4$) bond alternating $S = \frac{1}{2}$ anisotropic Heisenberg plaquette. Here, the stronger AFM bonds (J_1) are assumed between the site-pairs $(1, 2)$ and $(3, 4)$, while the FM or weaker AFM bonds (J_2) are acting between the site-pairs $(2, 3)$ and $(4, 1)$. The Hamiltonian has been diagonalised in different S_T^z sectors for obtaining analytic expressions of eigenvalues and eigenfunctions. Eigenvalues (e_i) are displayed in table 1. Ground state lies in $S_T^z = 0$ sector having energy e_0. The ground state wave function is given by $\Psi_0 = \frac{1}{\sqrt{1+X^2+Y^2}}(\psi_1 + X\psi_2 + Y\psi_3)$, where $\psi_1 = \frac{1}{\sqrt{2}}(\uparrow\uparrow\downarrow\downarrow + \downarrow\downarrow\uparrow\uparrow)$, $\psi_2 = \frac{1}{\sqrt{2}}(\uparrow\downarrow\uparrow\downarrow + \downarrow\uparrow\downarrow\uparrow)$,

Table 1. Eigenvalues in all S_{T}^z subspaces, where $a = \frac{2}{3}[(\Delta^2 + 3)(J_1^2 + J_2^2) - J_1 J_2 \Delta^2]^{1/2}$, $b = -\frac{J_1+J_2}{6}\Delta$ and $\phi = \arccos[3q/(ap)]$, $q = e_4(e_3 e_4 + J_1^2 - J_2^2) - \frac{e_3}{27}[2e_3^2 + 9(e_4^2 + J_1^2 + J_2^2)]$ and $p = -\frac{1}{3}[(\Delta^2 + 3)(J_1^2 + J_2^2) - J_1 J_2 \Delta^2]$.

S_{T}^z	Eigenvalues	S_{T}^z	Eigenvalues
0	$e_5 = -\frac{J_1-J_2}{2}\Delta$	1, −1	$e_9 = \frac{J_1+J_2}{2}$
	$e_4 = \frac{J_1-J_2}{2}\Delta$		$e_8 = \frac{-J_1+J_2}{2}$
	$e_3 = -\frac{J_1+J_2}{2}\Delta$		$e_7 = \frac{J_1-J_2}{2}$
	$e_2 = a\cos\frac{\phi}{3} + b$		$e_6 = -\frac{J_1+J_2}{2}$
	$e_1 = a\cos\frac{\phi+4\pi}{3} + b$	2, −2	$e_{10} = \frac{J_1+J_2}{2}\Delta$
	$e_0 = a\cos\frac{\phi+2\pi}{3} + b$		

$\psi_3 = \frac{1}{\sqrt{2}}(\uparrow\downarrow\downarrow\uparrow + \downarrow\uparrow\uparrow\downarrow)$, $X = \frac{e_0-e_4}{J_2}$ and $Y = X\frac{J_1}{e_0+e_4}$. Dimer order parameter is defined by the ground state expectation value [27],

$$O_{\mathrm{D}} = \langle\Psi_0|\vec{S}_i \cdot \vec{S}_{i+1} - \vec{S}_{i+1} \cdot \vec{S}_{i+2}|\Psi_0\rangle = \frac{1 - 2X - Y^2 + 2XY}{2(1 + X^2 + Y^2)}.$$

When $J_1 = J_2$, the ground state energy, $e_0 = -\frac{J_1}{2}(\Delta + \sqrt{8 + \Delta^2})$, and $O_{\mathrm{D}} = 0$ since $Y = 1$. On the FM region, when $J_2 = -J_1$, $e_0 = -J_1\sqrt{2 + \Delta^2}$, $O_{\mathrm{D}} = (1 - 2x - x^2/2)/[2(1 + x^2/2)]$, where $x = (\Delta + \sqrt{2 + \Delta^2})$. When $\Delta = 1$, ground state energy $e_0 = -\frac{1}{2}[J_1 + J_2 + \sqrt{(J_1 + J_2)^2 + 3(J_1 - J_2)^2}]$ and ground state wave function, $\Psi_0 = \frac{2}{\sqrt{1+c^2+d^2}}(c[14][32] + d[12][34])$, where, $c = \frac{J_2}{e_0-e_7}$, $d = \frac{J_1}{e_0+e_7}$ and the singlet, $[ij]$ is defined as

$$[ij] = \frac{1}{\sqrt{2}} \left(\underset{i}{\uparrow}\ \underset{j}{\downarrow}\ -\ \underset{i}{\downarrow}\ \underset{j}{\uparrow}\right).$$
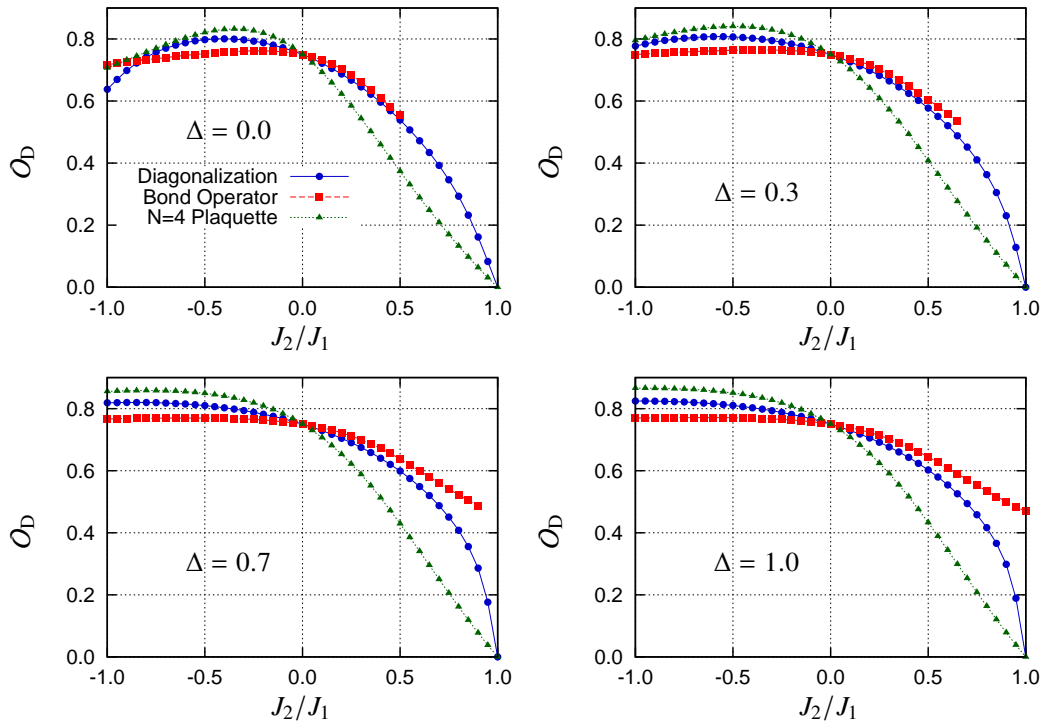
However, when $\Delta = 0$, ground state energy, $e_0 = -\sqrt{J_1^2 + J_2^2}$, and this is the same for both AFM and FM J_2 and ground state, $\Psi_0 = \frac{2e_0^0}{\sqrt{e_0^{0^2}+J_1^2+J_2^2}}(\frac{J_2}{e_0^0}[14][32] + \frac{J_1}{e_0^0}[12][34] - \frac{e_0^0+J_1+J_2}{\sqrt{2}e_0^0}\psi_2)$. Variations of O_{D} are shown in figure 1 in the green dotted lines and triangles. O_{D} vanishes exactly over the line $J_2/J_1 = 1.0$ and otherwise non-zero. It is observed that O_{D} calculated in this four-spin bond alternating plaquette, captures the true many-particle results closely.

3. Bond operator representation

In the bond operator formalism [28], two spin-$\frac{1}{2}$ operators, say, $\vec{S}_l$ and $\vec{S}_r$ around every AFM bond having exchange strength J_1 are expressed in terms of a singlet state $|s\rangle$ and three triplet states $|t_x\rangle$, $|t_y\rangle$, and $|t_z\rangle$ around the same bond. The singlet ($s^\dagger$) and triplet ($t_\alpha^\dagger$, $\alpha = x, y, z$) operators which create these states out of the vacuum state $|0\rangle$, are

$$|s\rangle = s^\dagger|0\rangle = \frac{1}{\sqrt{2}}(|\uparrow\downarrow\rangle - |\downarrow\uparrow\rangle),$$

$$|t_x\rangle = t_x^\dagger|0\rangle = -\frac{1}{\sqrt{2}}(|\uparrow\uparrow\rangle - |\downarrow\downarrow\rangle),$$

Figure 1. (Color online) Plots of dimer order as a function of J_2/J_1 for $\Delta = 0.0$, 0.3, 0.7, 1.0. Blue (solid line, circle), red (dashed line, square) and green (dotted line, triangle) correspond to the exact diagonalization, bond operator and $N = 4$ plaquette results, respectively. Bond operator lines terminate at those points where the convergence of self-consistent equations is not attained.

$$|t_y\rangle = t_y^\dagger |0\rangle = \frac{i}{\sqrt{2}} \left(|\uparrow\uparrow\rangle + |\downarrow\downarrow\rangle \right),$$

$$|t_z\rangle = t_z^\dagger |0\rangle = \frac{1}{\sqrt{2}} \left(|\uparrow\downarrow\rangle + |\downarrow\uparrow\rangle \right).$$

Only the singlet state changes sign upon interchanging the two spins in each bond. The components of spin operators, $\vec{S}_l$ and $\vec{S}_r$ can be expressed in terms of these singlet and triplet operators as

$$S_l^\alpha = \frac{1}{2} \left(s^\dagger t_\alpha + t_\alpha^\dagger s - i \epsilon_{\alpha\beta\gamma} t_\beta^\dagger t_\gamma \right),$$

$$S_r^\alpha = \frac{1}{2} \left(-s^\dagger t_\alpha - t_\alpha^\dagger s - i \epsilon_{\alpha\beta\gamma} t_\beta^\dagger t_\gamma \right), \tag{3.1}$$

where α, β and γ represent the x, y and z components and the Levi-Cività symbol, $\epsilon_{\alpha\beta\gamma}$ represents the totally anti-symmetric tensor. Summation over the repeated α, β and γ indices is henceforth assumed except stated otherwise. By considering the bosonic commutation relations, like

$$[s, s^\dagger] = 1, \qquad [t_\alpha, t_\beta^\dagger] = \delta_{\alpha\beta}, \qquad [s, t_\alpha^\dagger] = 0,$$

on a particular bond, one can reproduce the $S = \frac{1}{2}$, SU(2) commutation relations on a specific site, $[S^\alpha, S^\beta] = i \epsilon_{\alpha\beta\gamma} S^\gamma$. Similarly, by imposing the constraint, or the completeness relation,

$$s^\dagger s + t_\alpha^\dagger t_\alpha = 1, \tag{3.2}$$

on each bond, the value of spin in each site, say, $S_l^2 = S_r^2 = \frac{3}{4}$ is retained. Likewise, the anisotropic AFM bond can be expressed as

$$S_{2i-1}^x S_{2i}^x + S_{2i-1}^y S_{2i}^y + \Delta S_{2i-1}^z S_{2i}^z = E_s\, s_j^\dagger s_j + E_t^z\, t_{jz}^\dagger t_{jz} + E_t^\alpha\, t_{j\alpha}^\dagger t_{j\alpha},$$

where j represents the bond between the adjacent sites $2i - 1$ and $2i$, $\alpha = x, y$, $E_s = -(\frac{\Delta}{4} + \frac{1}{2})$ is the singlet while $E_t^z = (-\frac{\Delta}{4} + \frac{1}{2})$ along with the doubly degenerate $E_t^\alpha = \frac{\Delta}{4}$ are the triplet eigenvalues of the anisotropic bond. Substituting the operator representation of spins defined in equation (3.1) into the bond alternating Hamiltonian of equation (1.1) we have the form:

$$H = H_0 + H_1 + H_2,$$

$$H_0 = \sum_j \left[J_1 \left(E_s\, s_j^\dagger s_j + E_t^z\, t_{jz}^\dagger t_{jz} + E_t^\alpha\, t_{j\alpha}^\dagger t_{j\alpha} \right) - \mu \left(s_j^\dagger s_j + t_{jz}^\dagger t_{jz} + t_{j\alpha}^\dagger t_{j\alpha} - 1 \right) \right],$$

$$H_1 = -\frac{J_2}{4} \sum_j \left(s_j^\dagger s_{j+1} t_{j\alpha} t_{j+1\alpha}^\dagger + s_j s_{j+1} t_{j\alpha}^\dagger t_{j+1\alpha}^\dagger + t_{jz}^\dagger t_{j+1z}^\dagger t_{j\alpha} t_{j+1\alpha} - t_{jz}^\dagger t_{j+1z} t_{j\alpha} t_{j+1\alpha}^\dagger + \text{h.c.} \right),$$

$$H_2 = -\frac{J_2\Delta}{4} \sum_j \left(s_j^\dagger s_{j+1} t_{jz} t_{j+1z}^\dagger + s_j s_{j+1} t_{jz}^\dagger t_{j+1z}^\dagger + t_{jx}^\dagger t_{j+1x}^\dagger t_{jy} t_{j+1y} - t_{jx}^\dagger t_{j+1x} t_{jy} t_{j+1y}^\dagger + \text{h.c.} \right), \quad (3.3)$$

where the summation j runs over $N/2$ number of bonds. The portion of the Hamiltonian containing triple-t operators vanishes due to reflection symmetry [28]. Exploiting the translational invariance of the model, a site-independent parameter μ is introduced to take the constraint, equation (3.2) into care. Here, condensation of singlet boson is imposed, which means $\langle s_j \rangle = \bar{s}$. Parts of the Hamiltonian, H_1 and H_2, those containing quartic t operators are treated by using mean-field decoupling scheme. Four mean-field parameters (real) are

$$P_z = \langle t_{jz}^\dagger t_{j+1z} \rangle, \qquad P_\alpha = \langle t_{j\alpha}^\dagger t_{j+1\alpha} \rangle, \qquad Q_z = \langle t_{jz} t_{j+1z} \rangle \qquad \text{and} \qquad Q_\alpha = \langle t_{j\alpha} t_{j+1\alpha} \rangle. \quad (3.4)$$

Summation convention over α while defining P_α and Q_α is not applied. By performing Fourier transform of the operators $t_j = \sqrt{\frac{2}{N}} \sum_k t_k\, \mathrm{e}^{ikja}$, where a is the lattice constant, the approximated Hamiltonian can be written as

$$H_M = E_0 + \sum_k \left[\Lambda_{kz} t_{kz}^\dagger t_{kz} + \Lambda_{k\alpha} t_{k\alpha}^\dagger t_{k\alpha} + \Delta_{kz} (t_{kz} t_{-kz} + \text{h.c.}) + \Delta_{k\alpha} (t_{k\alpha} t_{-k\alpha} + \text{h.c.}) \right], \quad (3.5)$$

where

$$E_0 = \frac{N}{2} \left\{ \mu - \left[J_1 \left(\frac{\Delta}{4} + \frac{1}{2} \right) + \mu \right] \bar{s}^2 + J_2 \left[Q_\alpha Q_z - P_\alpha P_z + \frac{\Delta}{2} \left(Q_\alpha^2 - P_\alpha^2 \right) \right] \right\},$$

$$\Lambda_{kz} = J_1 \left(-\frac{\Delta}{4} + \frac{1}{2} \right) - \mu - \frac{J_2}{2} \left(\Delta\, \bar{s}^2 - 2P_\alpha \right) \cos(ka),$$

$$\Lambda_{k\alpha} = J_1 \frac{\Delta}{4} - \mu - \frac{J_2}{2} \left(\bar{s}^2 - P_z - \Delta\, P_\alpha \right) \cos(ka),$$

$$\Delta_{kz} = -\frac{J_2}{4} \left(\Delta\, \bar{s}^2 + 2Q_\alpha \right) \cos(ka), \qquad \Delta_{k\alpha} = -\frac{J_2}{4} \left(\bar{s}^2 + Q_z + \Delta\, Q_\alpha \right) \cos(ka).$$

The Hamiltonian, H_M can be easily diagonalized by introducing the four-component vector $\Psi_k = (t_{kz}^\dagger\ t_{k\alpha}^\dagger\ t_{-kz}\ t_{-k\alpha})$. Thus, H_M can be expressed as

$$H_M = E_0 - \frac{1}{2} \sum_k (\Lambda_{kz} + 2\Lambda_{k\alpha}) + \sum_k \Psi_k^\dagger H_k \Psi_k,$$

$$H_k = \begin{pmatrix} A_k & B_k \\ B_k & A_k \end{pmatrix}, \qquad A_k = \frac{1}{2} \begin{pmatrix} \Lambda_{kz} & 0 \\ 0 & \Lambda_{k\alpha} \end{pmatrix}, \qquad B_k = \begin{pmatrix} \Delta_{kz} & 0 \\ 0 & \Delta_{k\alpha} \end{pmatrix}.$$

In terms of bosonic operators, Bogoliubov transformation means diagonalization of the matrix $I_B H_k$, where

$$I_B = \begin{pmatrix} I & 0 \\ 0 & -I \end{pmatrix}, \quad \text{and} \quad I = \begin{pmatrix} 1 & 0 \\ 0 & 1 \end{pmatrix}.$$

The positive eigenvalues of the matrix, $I_B H_k$ are $\frac{1}{2}\omega_{kz}$ and $\frac{1}{2}\omega_{k\alpha}$, where $\omega_{kz} = \sqrt{\Lambda_{kz}^2 - 4\Delta_{kz}^2}$ and $\omega_{k\alpha} = \sqrt{\Lambda_{k\alpha}^2 - 4\Delta_{k\alpha}^2}$. In terms of a new four-component vector $\Phi_k^\dagger = (\gamma_{kz}^\dagger \; \gamma_{k\alpha}^\dagger \; \gamma_{-kz} \; \gamma_{-k\alpha})$, H_M looks like

$$H_M = E_0 - \frac{1}{2}\sum_k (\Lambda_{kz} + 2\Lambda_{k\alpha}) + \frac{1}{2}\sum_k \Phi_k^\dagger H_k^d \Phi_k,$$

$$H_k^d = \begin{pmatrix} \Omega_k & 0 \\ 0 & \Omega_k \end{pmatrix}, \qquad \Omega_k = \begin{pmatrix} \omega_{kz} & 0 \\ 0 & \omega_{k\alpha} \end{pmatrix}, \qquad \Phi_k = T_k \Psi_k,$$

$$T_k = \begin{pmatrix} u_k & v_k \\ v_k & u_k \end{pmatrix}, \qquad u_k = \frac{1}{\sqrt{2}}\begin{pmatrix} \sqrt{1 + \frac{\Lambda_{kz}}{\omega_{kz}}} & 0 \\ 0 & \sqrt{1 + \frac{\Lambda_{k\alpha}}{\omega_{k\alpha}}} \end{pmatrix}, \qquad v_k = \frac{1}{\sqrt{2}}\begin{pmatrix} \sqrt{-1 + \frac{\Lambda_{kz}}{\omega_{kz}}} & 0 \\ 0 & \sqrt{-1 + \frac{\Lambda_{k\alpha}}{\omega_{k\alpha}}} \end{pmatrix}.$$

H_M can further be expressed as

$$H_M = E_0 - \frac{1}{2}\sum_k (\Lambda_{kz} + 2\Lambda_{k\alpha} - \omega_{kz} - 2\omega_{k\alpha}) + \sum_k \left(\omega_{kz}\,\gamma_{kz}^\dagger \gamma_{kz} + \omega_{k\alpha}\,\gamma_{k\alpha}^\dagger \gamma_{k\alpha}\right). \tag{3.6}$$

Therefore, it turns out that ω_{kz} and $\omega_{k\alpha}$ are like the non-degenerate longitudinal and doubly-degenerate transverse branches of triplet dispersion relations, respectively. When $\Delta = 1$, the two branches merge to each other leading to a triply-degenerate single triplet branch. The parameters μ, $\bar{s}$, P_z, P_α, Q_z and Q_α are determined by solving the six saddle-point equations:

$$\left\langle \frac{\partial H_M}{\partial \mu} \right\rangle = 0, \quad \left\langle \frac{\partial H_M}{\partial \bar{s}} \right\rangle = 0, \quad \left\langle \frac{\partial H_M}{\partial P_z} \right\rangle = 0, \quad \left\langle \frac{\partial H_M}{\partial P_\alpha} \right\rangle = 0, \quad \left\langle \frac{\partial H_M}{\partial Q_z} \right\rangle = 0, \quad \left\langle \frac{\partial H_M}{\partial Q_\alpha} \right\rangle = 0,$$

which lead to the following six self-consistent equations at $T = 0$ K.

$$\mu = \frac{J_2}{2N}\sum_k \left(\Delta\,\frac{2\Delta_{kz} - \Lambda_{kz}}{\omega_{kz}} + 2\,\frac{2\Delta_{k\alpha} - \Lambda_{k\alpha}}{\omega_{k\alpha}} + \Delta + 2\right)\cos(ka) - J_1\left(\frac{\Delta}{4} + \frac{1}{2}\right),$$

$$\bar{s}^2 = \frac{5}{2} - \frac{1}{N}\sum_k \left(\frac{\Lambda_{kz}}{\omega_{kz}} + 2\,\frac{\Lambda_{k\alpha}}{\omega_{k\alpha}}\right),$$

$$P_z = \frac{1}{N}\sum_k \left(\frac{\Lambda_{kz}}{\omega_{kz}} - 1\right)\cos(ka),$$

$$P_\alpha = \frac{1}{N}\sum_k \left(\frac{\Lambda_{k\alpha}}{\omega_{k\alpha}} - 1\right)\cos(ka),$$

$$Q_z = -\frac{2}{N}\sum_k \frac{\Delta_{kz}}{\omega_{kz}}\cos(ka),$$

$$Q_\alpha = -\frac{2}{N}\sum_k \frac{\Delta_{k\alpha}}{\omega_{k\alpha}}\cos(ka). \tag{3.7}$$

For fixed values of J_1, J_2 and Δ, the six self-consistent solutions are obtained from equations (3.7) and are employed to determine the dispersion relations, ground state energy, spin gap and dimer order. For $J_2 = 0$, values of the parameters, P_z, P_α, Q_z and Q_α must be zero, and they are non-zero when $J_2 \neq 0$. The solutions for μ are always negative while those for $\bar{s}^2$ are always positive. These six self-consistent

equations are found to converge in most of the anisotropic parameter regions except the regime where spin gap is vanishingly small which occurs when $J_1 \approx J_2$ and $\Delta \approx 0$. So, the values of ground state energy, spin gap and dimer order in this regime are not plotted in the respective figures in subsequent sections. The ground state energy per site (E_G) is given by the following expression,

$$E_G = \frac{E_0}{N} - \frac{1}{2N} \sum_k (\Lambda_{kz} + 2\Lambda_{k\alpha} - \omega_{kz} - 2\omega_{k\alpha}).$$

For $J_1 = J_2$ and $\Delta = 1$, $E_G = -0.45130123 J_1$, which is only 0.18% lower than the exact Bethe-Ansatz result, i.e., $(0.25 - \ln 2)J_1 = -0.44314718 J_1$. The values of E_G are very close to the exact diagonalization results in the entire parameter regime except the point $\Delta = 0$ and those are shown in figure 2.

The expression of ground state dimer order looks like

$$\langle O_D \rangle = D_0 - \frac{1}{2} \sum_k \left(X_{kz} + 2X_{k\alpha} + \frac{\Lambda_{kz} X_{kz} - 4\Delta_{kz} Y_z}{\omega_{kz}} + 2\frac{\Lambda_{k\alpha} X_{k\alpha} - 4\Delta_{k\alpha} Y_\alpha}{\omega_{k\alpha}} \right),$$

$$D_0 = -\frac{3}{4}\bar{s}^2 + P_z P_\alpha - Q_z Q_\alpha + \frac{1}{2}\left(P_\alpha^2 - Q_\alpha^2\right),$$

$$X_{kz} = \frac{1}{4}\left[1 + 2(\bar{s}^2 - 2P_\alpha)\cos(ka)\right], \qquad X_{k\alpha} = \frac{1}{4}\left[1 + 2(\bar{s}^2 - P_z - P_\alpha)\cos(ka)\right],$$

$$Y_z = \frac{1}{4}\left(\bar{s}^2 + 2Q_\alpha\right), \qquad Y_\alpha = \frac{1}{4}\left(\bar{s}^2 + Q_z + Q_\alpha\right).$$

The values of this O_D along with plaquette and exact diagonalization results are shown in figure 1. Bond operator results are discontinued at those points where convergence fails to be attained.
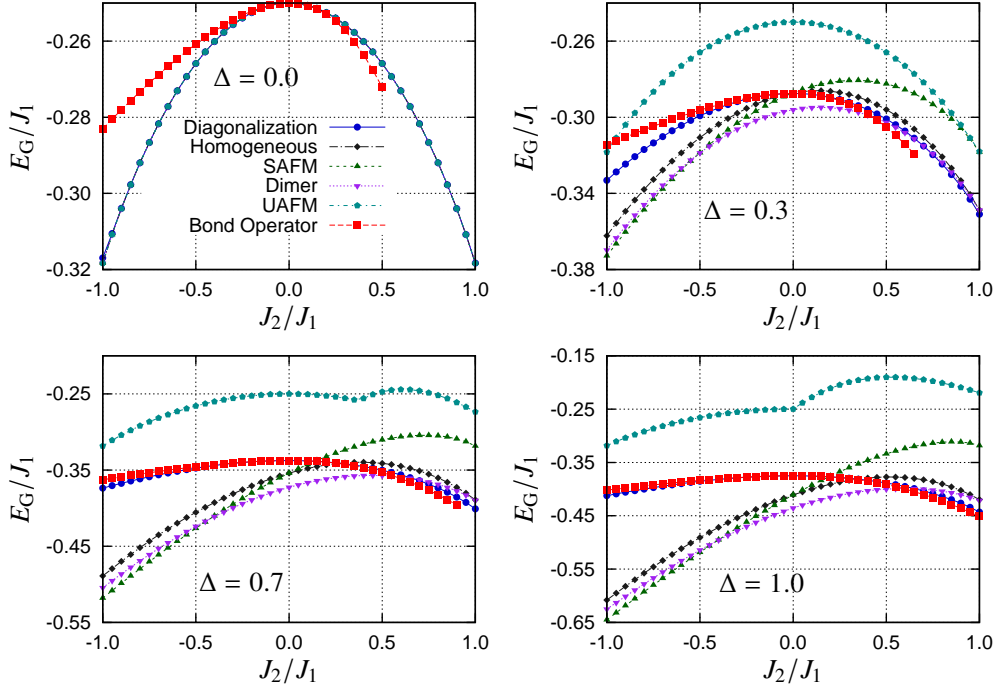

Figure 2. (Color online) Plots of ground state energy per site as a function of J_2/J_1 for $\Delta = 0.0, 0.3, 0.7, 1.0$. Blue (solid line, circle) corresponds to the exact diagonalization data. Red (dashed line, square) corresponds to the bond operator result. Different Jordan-Wigner based mean-field results: UAFM (dark-cyan, dashed-dot line, pentagon), homogeneous (black, dashed-dot line, diamond), SAFM (green, dashed line, triangle) and dimer (purple, dotted line, inverted triangle). Bond operator lines terminate at those points where the convergence of self-consistent equations is not attained.

The dispersion relations, ω_{kz} and $\omega_{k\alpha}$ arising from the excitations of spin-triplet states are shown in figure 3. $J_2 = 0$ is a dispersionless point, where both ω_{kz} and $\omega_{k\alpha}$ are flat since energy propagation is impossible in the absence of inter-bond interaction J_2. This particular point is not shown in figure 3. For $\Delta = 0$, ω_{kz} is almost flat with small curvature, concave down for AFM J_2 while concave up for FM J_2, whereas, $\omega_{k\alpha}$ has the maximum curvature. ω_{kz} will be perfect dispersionless if the part of the Hamiltonian [equation (3.3)] containing four-t operators is neglected. It is interesting to note that even though $\Delta = 0$, ω_{kz} is non-zero. So, it establishes the fact that the existence of longitudinal mode is quantum mechanically possible in the absence of the longitudinal part of the Hamiltonian. These modes hardly participate in energy propagation. However, in general, both ω_{kz} and $\omega_{k\alpha}$ are concave up for AFM J_2 and concave down for FM J_2. Bandwidth for ω_{kz} ($\omega_{k\alpha}$) increases (decreases) with increasing Δ for fixed value of J_2. On the other hand, bandwidths for ω_{kz} as well as $\omega_{k\alpha}$ increase with increasing value of both AFM and FM J_2 for fixed value of Δ. However, for a fixed value of AFM J_2, bandwidths
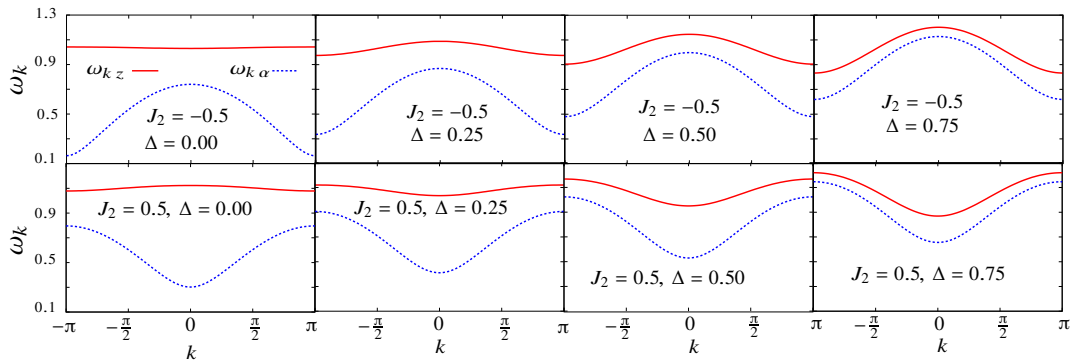
Figure 3. (Color online) Dispersion relations (in unit of J_1) with respect to k. ω_{kz} and $\omega_{k\alpha}$ are in red (solid) and blue (dashed) lines, respectively.
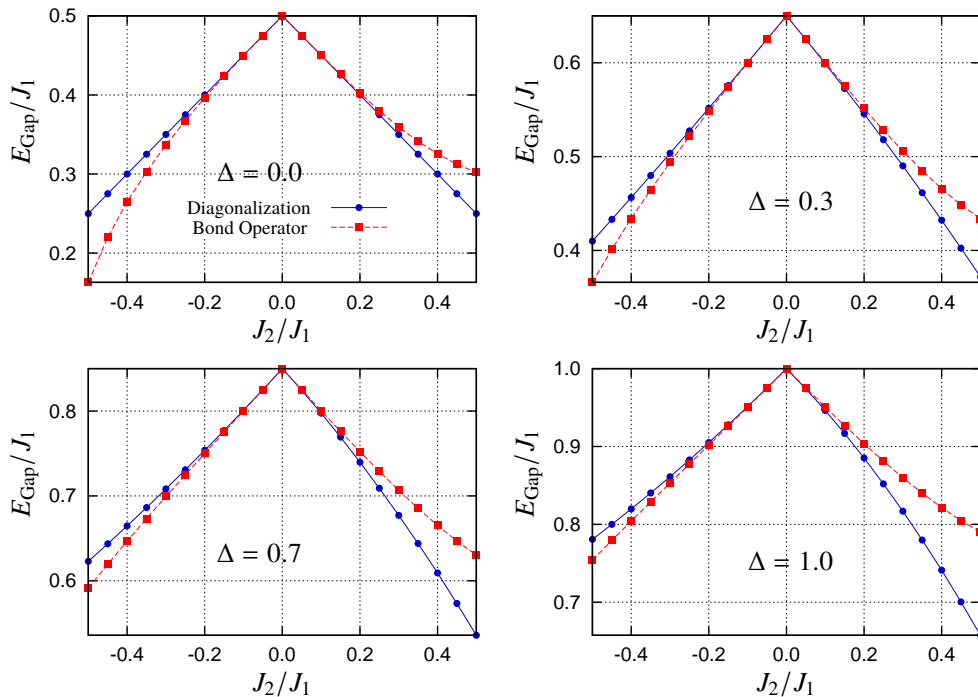
Figure 4. (Color online) Plots of E_{Gap}/J_1 with respect to J_2/J_1. Blue (solid line, circle) and red (dashed line, square) correspond to the exact diagonalization and bond operator results, respectively.

for $\omega_{k\,z}$ and $\omega_{k\,\alpha}$ are separately the same to them for that value of FM J_2 for a definite value of Δ. The minima of triplet dispersion relations, $\omega_{k\,z}$ and $\omega_{k\,\alpha}$ are found at $k = 0$ when $J_2 > 0$ and at $k = \pi$ when $J_2 < 0$ as far as $|J_2| \leqslant J_1$. So, the value of spin gap can be estimated by using the relations, $E_{\text{Gap}} = \min[\omega_{k\,z}(k = 0), \omega_{k\,\alpha}(k = 0)]$ when $J_2 > 0$ and $E_{\text{Gap}} = \min[\omega_{k\,z}(k = \pi), \omega_{k\,\alpha}(k = \pi)]$ when $J_2 < 0$. Since $\omega_{k\,\alpha} \leqslant \omega_{k\,z}$ for any value of the wave vector, k, in the anisotropic parameter regime $0 \leqslant \Delta \leqslant 1$, $E_{\text{Gap}} = \omega_{k\,\alpha}(k = 0)$ for AFM J_2 and $E_{\text{Gap}} = \omega_{k\,\alpha}(k = \pi)$ for FM J_2. Figure 3 shows that the value of E_{Gap} increases with the increase of Δ in every case. Variation of E_{Gap} with J_2/J_1 is shown in figure 4 along with the exact diagonalization results. E_{Gap} is found to decrease in the absence of the part of equation (3.3) containing four-t operators terms.

4. Jordan-Wigner representation

This model is exactly solvable in terms of Fermi gas of spinless fermions for $\Delta = 0$ by using the Jordan-Wigner transformation [29]

$$S_i^+ = c_i^\dagger e^{i\pi \sum_{j=1}^{i-1} \hat{n}_j},$$

$$S_i^- = e^{-i\pi \sum_{j=1}^{i-1} \hat{n}_j} c_i,$$

$$S_i^z = \hat{n}_i - \frac{1}{2},$$

where c_i and $c_i^\dagger$ are the spinless fermion annihilation and creation operators, respectively. $\hat{n}_i = c_i^\dagger c_i$ is the usual fermion number operator. This bond alternating system has a translational symmetry of two lattice units and so it becomes useful to introduce two types of spinless fermions defined on odd and even lattice sites by relabeling them as: $c_i = a_i$ for odd sites and $c_i = b_i$ for even sites. As a result, the Hamiltonian becomes

$$H = \sum_{i=1,3,5,\ldots} \left[\frac{J_1}{2} \left(a_i^\dagger b_{i+1} + b_{i+1}^\dagger a_i \right) + J_1 \Delta \left(a_i^\dagger a_i - \frac{1}{2} \right) \left(b_{i+1}^\dagger b_{i+1} - \frac{1}{2} \right) \right]$$
$$+ \sum_{i=1,3,5,\ldots} \left[\frac{J_2}{2} \left(b_{i+1}^\dagger a_{i+2} + a_{i+2}^\dagger b_{i+2} \right) + J_2 \Delta \left(b_{i+1}^\dagger b_{i+1} - \frac{1}{2} \right) \left(a_{i+2}^\dagger a_{i+2} - \frac{1}{2} \right) \right]. \quad (4.1)$$

For $\Delta \neq 0$, four-operator terms can be treated by the mean-field analysis. By allowing contractions of types, say, $C_a = \langle a_i^\dagger b_{i+1} \rangle$ and $C_b = \langle b_i^\dagger a_{i+1} \rangle$, the mean-field Hamiltonian in momentum space reads as

$$H_{\text{MF}} = \sum_k \left[C_k a_k^\dagger b_k + \bar{C}_k b_k^\dagger a_k + h \left(a_k^\dagger a_k - b_k^\dagger b_k \right) \right] + \frac{N\Delta}{8}(J_1 + J_2) + \frac{N\Delta}{2} \left(J_1 |C_a|^2 + J_2 |C_b|^2 \right), \quad (4.2)$$

where $C_k = (\frac{J_1}{2} - J_1 \Delta C_a) e^{-ika} + (\frac{J_2}{2} - J_2 \Delta C_b) e^{ika}$ and $h = \frac{\Delta}{2}(J_1 - J_2)$. In this fermionic description, h acts as a chemical potential whose value is the same for every particle but opposite in sign for two different kinds of particles, say, positive for a and negative for b. In other words, h acts as a staggered field giving rise to a periodic potential experienced by the particles with the periodicity of two lattice units. As a result, Brillouin zone shrinks to its half yielding a spin gap in its boundary. On the other hand, h vanishes for the uniform bond strength, i.e., when $J_1 = J_2$ and so the spin gap.

By using the fermionic Bogoliubov transformation

$$a_k = u_k \alpha_k + v_k \beta_k, \qquad b_k = -v_k^* \alpha_k + u_k^* \beta_k,$$

where $u_k = r\, e^{i\theta_k}$, $v_k = r' e^{i\theta_k}$ and $e^{2i\theta_k} = C_k/|C_k|$, the diagonalized mean-field Hamiltonian looks like

$$H_{\text{MF}} = \sum_k E(k) \left(\alpha_k^\dagger \alpha_k - \beta_k^\dagger \beta_k \right) + \frac{N\Delta}{8}(J_1 + J_2) + \frac{N\Delta}{2} \left(J_1 |C_a|^2 + J_2 |C_b|^2 \right), \quad (4.3)$$

where $E(k) = \sqrt{h^2 + |C_k|^2}$.

By allowing contractions of other possible ways, say, $D_a = \langle a_i^\dagger a_i - \frac{1}{2}\rangle$ and $D_b = \langle b_{i+1}^\dagger b_{i+1} - \frac{1}{2}\rangle$, the mean-field Hamiltonian in momentum space becomes

$$H_{\mathrm{MF}} = \sum_k \left[D_k\, a_k^\dagger b_k + \bar{D}_k\, b_k^\dagger a_k + \Delta\,(J_1 + J_2)\left(D_b\, a_k^\dagger a_k + D_a\, b_k^\dagger b_k \right) \right]$$
$$- \frac{N}{4}\Delta(J_1 + J_2)\,(D_a + D_b + 2D_a D_b), \tag{4.4}$$

where $D_k = \frac{1}{2}\left(J_1\,\mathrm{e}^{-\mathrm{i}ka} + J_2\,\mathrm{e}^{\mathrm{i}ka} \right)$. By performing the same Bogoliubov transformation, diagonalized Hamiltonian reads as

$$H_{\mathrm{MF}} = \sum_k \omega(k)\left(\alpha_k^\dagger \alpha_k - \beta_k^\dagger \beta_k \right) - \frac{N}{2}\,D\,h, \tag{4.5}$$

where $\omega(k) = \sqrt{h^2 + |D_k|^2}$ and $h = -\Delta(J_1 + J_2)D$, when $D_a = -D_b = D$.

The mean-field parameters, C_a, C_b, and D will be determined by solving self-consistent equations defined in the four different phases [30].

i) Paramagnetic (homogeneous) phase: when $C_a = C_b$ [8],

$$C_a = -\frac{1}{N}\sum_k \frac{\cos^2(ka)}{E(k)} \left[\left(\frac{J_1 + J_2}{2} \right)(1 - 2\,\Delta\,C_a) \right] \left[n_\beta(k) - n_\alpha(k) \right]. \tag{4.6}$$

ii) Staggered AFM (SAFM) phase: when $C_a = -C_b$,

$$C_a = \frac{1}{N}\sum_k \frac{\sin^2(ka)}{E(k)} \left[\left(\frac{J_1 - J_2}{2} \right)(1 - 2\,\Delta\,C_a) \right] \left[n_\beta(k) - n_\alpha(k) \right]. \tag{4.7}$$

iii) Alternating NN hopping (dimer) phase: when $C_a = \eta + \delta$ and $C_b = \eta - \delta$,

$$\eta = -\frac{1}{N}\sum_k \frac{\cos^2(ka)}{E(k)} \left[\left(\frac{J_1 + J_2}{2} \right)(1 - 2\Delta\eta) - \delta\Delta(J_1 - J_2) \right] \left[n_\beta(k) - n_\alpha(k) \right],$$
$$\delta = \frac{1}{N}\sum_k \frac{\sin^2(ka)}{E(k)} \left[\left(\frac{J_1 - J_2}{2} \right)(1 - 2\Delta\eta) - \delta\Delta(J_1 + J_2) \right] \left[n_\beta(k) - n_\alpha(k) \right]. \tag{4.8}$$

iv) Uniform AFM (UAFM) phase: when $D_a = -D_b$,

$$1 = \frac{1}{N}\sum_k \frac{\Delta(J_1 + J_2)}{\omega(k)} \left[n_\beta(k) - n_\alpha(k) \right]. \tag{4.9}$$

D_a vanishes when $J_1 = -J_2$. Another choice $D_a = D_b$, which corresponds to the uniform FM phase gives rise to $D_a = 0$. So, this choice does not produce a non-trivial result, and thus deserves no further attention. $n_\alpha(k) = \langle \alpha_k^\dagger \alpha_k \rangle$ and $n_\beta(k) = \langle \beta_k^\dagger \beta_k \rangle$ are the fermionic occupation probabilities at temperature T. At zero temperature, only the negative energy states are filled up, so, $n_\alpha(k) = 0$ and $n_\beta(k) = 1$. In this situation, the expressions of E_{G} can be written down easily for each mean-field case. For example, in the dimer phase (iii), it is given by

$$E_{\mathrm{G}} = -\frac{1}{\pi}\int_0^{\pi/2} E_k\,\mathrm{d}k + \frac{\Delta}{2}\left[J_1(\eta + \delta)^2 + J_2(\eta - \delta)^2 \right] + \frac{\Delta}{8}\,(J_1 + J_2).$$

For $\Delta = 0$, ground state energy can be exactly evaluated for any values of both $\frac{J_2}{J_1}$ and temperatures. For example, at $T = 0$, $E_{\mathrm{G}} = -\frac{1}{\pi}J_1 = -0.31830989 J_1$, when $\frac{J_2}{J_1} = 1$ and $\Delta = 0$.

This mean-field ground state energy has been improved by considering the second order contribution attributed to the fluctuations around the mean field. This correction may be evaluated by using the standard expression at $T = 0$ [31],

$$\Delta E = \sum_f \frac{|\langle g \, |(H - H_{\text{MF}})| \, f \rangle|^2}{E_g - E_f}, \qquad (4.10)$$

where $|g\rangle = \prod_k \beta_k^\dagger |0\rangle$ and $|f\rangle = \alpha_{k_1+q}^\dagger \alpha_{k_2-q}^\dagger |0\rangle$ are the ground state and the excited states of H_{MF}, respectively. The state $|f\rangle$ has two excited particles at wave vectors $k_1 + q$ and $k_2 - q$ at the positive energy branch. Non-zero contributions come from the four-operator terms in equation (4.1). Numerical evaluation of equation (4.10) leads to $\Delta E = -0.0171 J_1$ per site for $\frac{J_2}{J_1} = 1$ and $\Delta = 1$. The final value of the ground state energy is $E_G(\Delta = 1, J_1 = J_2) = -0.4367 J_1$, after the second order correction which is very close to the exact Bethe-Ansatz result, i.e., $-0.4431 J_1$.

The mean-field ground state energies have been plotted along with the exact diagonalization and bond operator results in the figure 2. Different Jordan-Wigner based mean-field results are UAFM (dark-cyan, dashed-dot line, pentagon), homogeneous (black, dashed-dot line, diamond), SAFM (green, dashed line, triangle) and dimer (purple, dotted line, inverted triangle). For $\Delta = 0$, Jordan-Wigner representation provides the exact ground state energy and thus it coincides with the exact diagonalization result (figure 2). However, when $\Delta > 0$, SAFM and UAFM phases do not at all agree with the exact diagonalization results. E_G evaluated in the UAFM phase is always higher, while that evaluated in SAFM phase is higher (lower) when J_2 is AFM (FM). Dimer and homogeneous phases do agree with the exact diagonalization result only in the AFM J_2 region. On the other hand, E_G evaluated in the bond operator formalism mostly coincides with the exact diagonalization result apart from the point $\Delta = 0$. For $\Delta = 0$, E_G derived in this formalism coincides with the exact diagonalization result around $|J_2/J_1| \approx 0$.

5. Exact diagonalization results

The ground state energy, spin gap and several ground state correlation functions have been obtained numerically at zero temperature. Ground state energy has been compared with the theoretical results. The spin gap is defined as the difference between the energies of ground state and the lowest excited state for a chain of finite number of spins. The Lanczos exact diagonalization technique is the most suitable algorithm when a few extreme eigenvalues are required. To find the ground state energy, the Hamiltonian is diagonalized in a subspace where $S_T^z = 0$. The Hilbert space is further reduced by exploiting two different symmetries of this Hamiltonian. The first one is the translational invariance of two lattice units while the second one is the spin inversion in every site. Due to the spin inversion symmetry, the energy eigenvalues satisfy the relation, $E(S_T^z) = E(-S_T^z)$. The periodic boundary condition is taken into account in every case. As a result, two different momentum wave vectors, $qT2$ and qR are defined to associate the symmetries of Hamiltonian with the translation of two lattice units and the spin inversion, respectively. Eventually, including those symmetries in the modified Lanczos algorithm [32], this computational procedure could find the eigenenergies of the spin chain up to the length (N) of 32 sites. The ground state is unique and corresponds to the wave vectors $qT2 = 0$ and $qR = \pi \, modulo \, (N, 4)$ for both AFM and FM J_2. The doubly degenerate lowest excited state corresponds to the $S_T^z = \pm 1$ and $qT2 = 0$ but $qR = 0$ for AFM J_2 while $qR = \frac{4\pi}{N} \, quotient \, (N, 4)$ for FM J_2. The Hamiltonian, H, [equation (1.1)] exhibits another useful symmetry in which the unitary operator, $U = \prod_j \exp(i\pi j S_j^z)$ transforms H as $U H(J_1, J_2, \Delta) U^\dagger = H(-J_1, -J_2, -\Delta)$. This symmetry transformation leads to the following result: when $\Delta = 0$, $U H(J_1, J_2, \Delta = 0) U^\dagger = -H(J_1, J_2, \Delta = 0)$. So, energy spectrum of H has the reflection symmetry around the zero energy. This symmetry is observed in the energy spectrum for $\Delta = 0$ and is shown in figure 5. The spectrum for $\Delta = 0$ is also symmetric around the point $J_2 = 0$, although no transformation is found to justify this symmetry. Obviously those symmetries are lost when $\Delta \neq 0$.

The full energy spectra of this model for four different values of Δ are plotted with respect to J_2/J_1 and are shown in figure 5 in which the uniqueness of the ground state and finite spin gap has been observed clearly. For $\Delta = 0$, the spectrum is symmetric around zero energy, but the spectra move toward
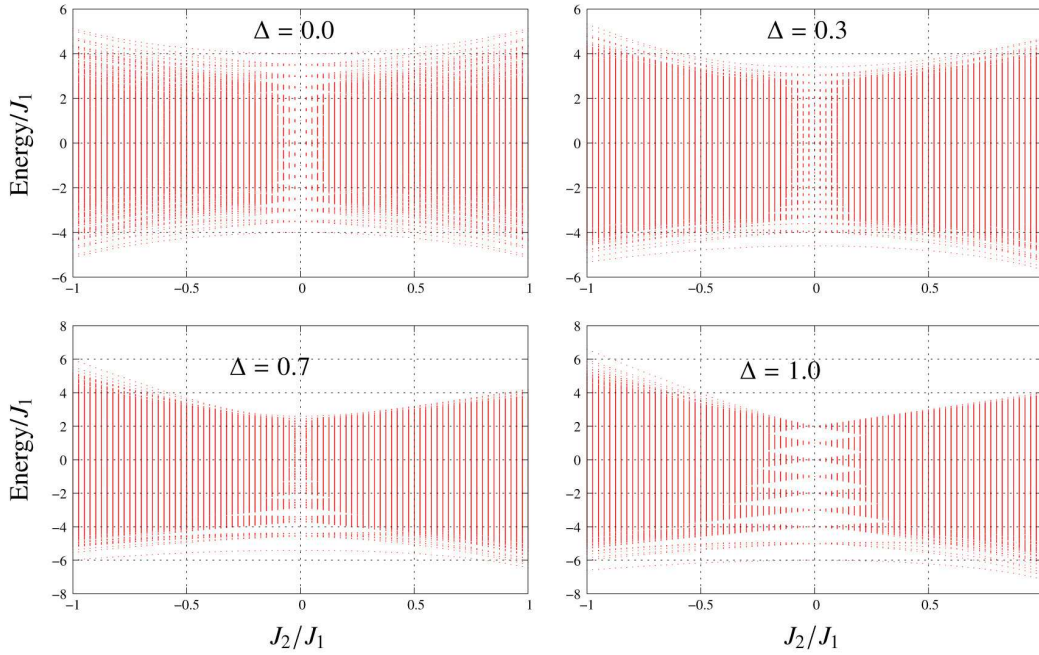
Figure 5. (Color online) Plot of all energies (in unit of J_1) with respect to J_2/J_1 for $\Delta = 0.0$, $\Delta = 0.3$, $\Delta = 0.7$, $\Delta = 1.0$ and $N = 16$. With the increasing Δ, the width of the energy band increases and moves toward the low energy side.

low energy side and at the same time symmetry is lost when $\Delta \neq 0$. The spectra are found to split into several bands around $J_2 = 0$. The number of bands increases with a decreasing Δ. The nature of those energy spectra remains unaltered in the open boundary condition.

To examine the effect of non-uniformity of the alternating bond strength on the spin gap, the modified Lanczos algorithm is employed designed for finite-size spin chain having integral multiple of 4, $N = 16, 20, \ldots, 32$. Ground state energy per site as well as spin gap depend on both the chain length (N) and the relative difference between alternating bond strengths, i.e., $\delta = (J_1 - J_2)/J_1$. The spin gap is defined as

$$E_{\text{Gap}}(N, \Delta, \delta) = E_{\text{F}}\left(N, \Delta, \delta, S_{\text{T}}^z = \pm 1\right) - E_{\text{Gr}}\left(N, \Delta, \delta, S_{\text{T}}^z = 0\right), \tag{5.1}$$

where E_{Gr} and E_{F} are the ground state and the first excited state energies, respectively. For $\delta = 0$, the spectrum is gapless for the entire range of $0 \leqslant \Delta \leqslant 1$, for AFM J_2 whereas, spin gap is found to develop as soon as $\delta \neq 0$ for the same range of Δ and AFM J_2. Thus, $\delta = 0$ serves as the critical point for this transition. On the other hand, for FM J_2, this spin gap is observed for any value of δ and Δ. The spin gap has been estimated by using several values of δ and Δ within the range $0 < \delta \leqslant 0.10$ and $0 < \Delta \leqslant 1.0$ for the chain lengths those are integral multiple of 4, i.e., $N = 16, 20, \ldots, 32$.

To obtain the values of E_{G} and E_{Gap} in large N limit, finite size extrapolations have been performed by using the Vanden-Broeck-Schwartz (VBS) algorithm [33] with $\alpha_{\text{VBS}} = -1$ in addition to the Bulirsch-Stoer (BST) algorithm [34]. Comparisons of those estimates with theoretical results reveal that the VBS algorithm yields more accurate values for both E_{G} and E_{Gap} than the BST algorithm. For the extrapolations, the values of E_{G} and E_{Gap} for chains of five different lengths like $N = 16, 20, \ldots, 32$ are considered. The extrapolated value of E_{G} agrees with the exact result up to the sixth decimal positions. For example, when $\Delta = 1$ and $\delta = 0$, the extrapolated value of ground state energy per site is $-0.44314728 J_1$ which is extremely close to the exact Bethe-Ansatz value, $-0.44314718 J_1$ or thus only 0.0000225% lower than the exact value. On the other extreme point, i.e., when $\Delta = 0$ and $\delta = 0$, the extrapolated value of E_{G} is $-0.31830988 J_1$ which completely agrees with the exact value $-J_1/\pi = -0.31830988 J_1$. Therefore, it is expected that the accuracy of those numerical estimations is very high. The extrapolated values of E_{Gap} are found by using the VBS algorithm and are plotted in figure 6 (a). This three-dimensional plot
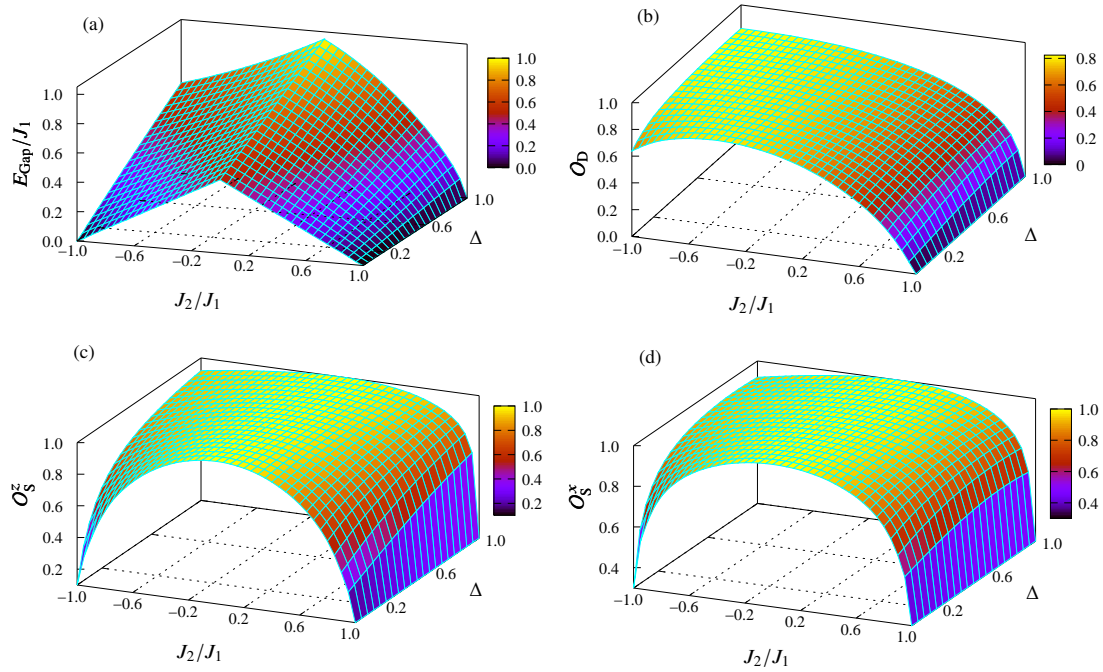
Figure 6. (Color online) Three dimensional plots of E_{Gap}/J_1 (a), O_{D} (b), O_{S}^z (c) and O_{S}^x (d) with respect to both J_2/J_1 and Δ.

reveals that E_{Gap} vanishes over the line $J_2/J_1 = 1$ and on the point, $J_2/J_1 = -1$, $\Delta = 0$. E_{Gap} is found to increase with the increase of both δ and Δ up to the line $J_2/J_1 = 0$. However, it again decreases toward FM region. The magnitude of spin gap is symmetric around $J_2 = 0$ for $\Delta = 0$, due to the symmetry of energy spectrum.

6. Ground state properties

The results obtained using various methods in the previous sections are summarized here. A comparison of values of E_{G} obtained in exact diagonalization, bond operator formalism and various Jordan-Wigner based mean-field methods has been displayed in figure 2. It shows that the values of E_{G} obtained in exact diagonalization and bond operator based mean-field formalism agree remarkably when $\Delta > 0$ while Jordan-Wigner based mean-field methods totally disagree. On the other hand, for $\Delta = 0$, Jordan-Wigner based exact result coincides with the exact diagonalization value but the results obtained by bond operator formalism show a qualitative agreement. Thus, it reveals that these two different analytic formalisms, bond operator and Jordan-Wigner, predict the true values of E_{G} in two different regions for these bond alternating models.

Ground state expectation value of the dimer order, O_{D}, has been evaluated numerically. In this expression, the stronger AFM bonds (J_1) are assumed between the sites i and $i + 1$ while the FM or weaker AFM bonds (J_2) are acting between the sites $i + 1$ and $i + 2$. The variation of O_{D} with respect to both Δ and J_2/J_1 has been shown in figure 6 (b). The values of O_{D} obtained by using exact diagonalization, bond operator formalism and four-spin plaquette have been shown in figure 1. All the methods show a good qualitative agreement. However, the bond operator based results do not vanish over the line $J_1 = J_2$. The exact diagonalization results quite agree with the DMRG results reported earlier by Watanabe and Yokoyama for $\Delta = 1$ [22]. O_{D} should vanish over the line $J_1 = J_2$ for an obvious reason but otherwise non-zero. O_{D} is found to increase steadily in AFM J_2 region and finally gets saturated in the FM region at the isotropic point, $\Delta = 1$. On the other hand, it decreases continuously in the anisotropic region towards the lower values of Δ. Variations of E_{Gap} with J_2/J_1 obtained by exact diagonalization and bond operator

formalism are shown in figure 4. Exact diagonalization results show that E_{Gap} vanishes over the line $J_1 = J_2$. Once again, bond operator formalism fails to estimate the value of E_{Gap} close to the line $J_1 = J_2$. It always predicts a non-zero value of E_{Gap} over this line for any value of Δ. In addition, this formalism underestimates (overestimates) the value of E_{Gap} in FM (AFM) J_2 region.

In order to characterize the Haldane phase in $S = 1$ Heisenberg chain, string correlation functions $O_{\text{S}}^{\alpha}(i - j)$ and string order parameter O_{S}^{α} have been introduced by den Nijs and Rommelse [3] and Tasaki [4] and those are defined as

$$O_{\text{S}}^{\alpha}(i - j) = -\langle S_i^{\alpha} \, e^{i\pi(S_{i+1}^{\alpha} + S_{i+2}^{\alpha} + \ldots + S_{j-1}^{\alpha})} \, S_j^{\alpha} \rangle,$$
$$O_{\text{S}}^{\alpha} = \lim_{|i-j| \to \infty} O_{\text{S}}^{\alpha}(i - j), \qquad \text{where} \qquad \alpha = x, y, z.$$

Here, S_i^{α} is the α-component of the spin operator S_i with the unity magnitude at the i-th site. The $S = \frac{1}{2}$ bond alternating Heisenberg chain can be mapped onto the isotropic AFM $S = 1$ Heisenberg chain when $J_2 \to -\infty$ and $\Delta = 1$ [15]. Hida also pointed out that bond alternating Hamiltonian with anisotropic ($\Delta \neq 1$) J_1 bond and isotropic ($\Delta = 1$) J_2 bond can be mapped onto the anisotropic AFM $S = 1$ Heisenberg chain when $J_2 \to -\infty$ [35]. In the same way, string correlation functions can be expressed in terms of $S = \frac{1}{2}$ operators as [36]

$$O_{\text{S}}^{\alpha}(i - j) = -4\langle S_{2i}^{\alpha} \, e^{i\pi(S_{2i+1}^{\alpha} + S_{2i+2}^{\alpha} + \ldots + S_{2j-2}^{\alpha})} \, S_{2j-1}^{\alpha} \rangle, \qquad \alpha = x, y, z. \tag{6.1}$$

In our model, $O_{\text{S}}^{x}(i - j) = O_{\text{S}}^{y}(i - j)$ due to the U(1) symmetry of the Hamiltonian, equation (1.1). Values of $O_{\text{S}}^{\alpha}(m)$ for $m = 1, 2, 3, \ldots, 8$ have been estimated numerically on a chain length of $N = 32$. O_{S}^{α} has been obtained by using the VBS algorithm for extrapolation out of these $O_{\text{S}}^{\alpha}(m)$ values. For $\Delta = 0$, O_{S}^{α} are symmetric about $J_2 = 0$, although this symmetry is lost for $\Delta \neq 0$. The value of O_{S}^{z} agrees with the previous estimation for $\Delta = 1$ [15]. $O_{\text{S}}^{z} = O_{\text{S}}^{x}$ when $\Delta = 1$. Variations of O_{S}^{z} and O_{S}^{x} have been shown in figure 6 (c) and (d), respectively. A qualitative similarity is found in their behaviours even in the anisotropic region. Both O_{S}^{z} and O_{S}^{x} are found to decrease rapidly when J_2/J_1 approaches 1.0, and ultimately vanish exactly over the line $J_2/J_1 = 1$. Coexistence of dimer order and string orders are found throughout the anisotropic region in this bond alternating Heisenberg chain barring the point $J_2/J_1 = -1$, $\Delta = 0$. The spin gap along with the string orders are found to vanish at the point, $J_2/J_1 = -1$, $\Delta = 0$, although the dimer order does not. So, it establishes the fact that the Haldane phase not only exists in bond alternating Heisenberg chain at the isotropic point, $J_2/J_1 \neq 1$, $\Delta = 1$ as predicted by Hida [15] but also in most of the anisotropic regions, $J_2/J_1 \neq 1$, $0 \leqslant \Delta < 1$. In addition, the only point in the anisotropic region where the Haldane phase does not survive is $J_2/J_1 = -1$, $\Delta = 0$. Therefore, apart from the FM point $J_2/J_1 = -1$, $\Delta = 0$ and AFM line $J_2/J_1 = 1$, $0 \leqslant \Delta \leqslant 1$, the Haldane phase exists in the whole parameter regime. It would be worth mentioning that for FM J_2 and $0 < \Delta \leqslant 1$, all the parameters, such as spin gap, dimer and string orders decrease with an increase of $|J_2/J_1|$ beyond the value $J_2/J_1 = -1$. The nature of decay of those parameters (figure 6) indicates that they all will vanish at larger values of $|J_2/J_1|$ in FM J_2 region. Therefore, this result hints at the collapse of Haldane phase for larger values of $|J_2/J_1|$ in the full anisotropic region. Thus, it is expected that either Néel or chiral ordered phase may appear in the region $|J_2/J_1| \gg 1$, and $0 \leqslant \Delta \leqslant 1$, by replacing the Haldane phase. However, this case is not considered in this study.

7. Conclusions

In this work, ground state properties, dispersion relations and spin gap of a bond alternating anisotropic $S = \frac{1}{2}$ Heisenberg chain have been evaluated for both the AFM-FM and AFM-AFM cases and in the full anisotropic regime $0 \leqslant \Delta \leqslant 1$. Both analytic (bond operator and Jordan-Wigner formulations) and numerical methods are employed to study those properties. Bond operator and Jordan-Wigner formulations provide more accurate results in two different parameter regimes. Ground state energy, dispersion relations, dimer order and spin gap have been derived by bond operator formalism. Longitudinal and transverse modes of dispersion relations are found. Longitudinal mode is found to survive even in

the absence of longitudinal part in the Hamiltonian. For $\Delta = 0$, the exact value of ground state energy has been derived by using the Jordan-Wigner representation. Meanwhile, for $\Delta \neq 0$, the ground state energy has been derived by using the Jordan-Wigner based mean-field theory. Those theoretical values have further been supplemented by the exact diagonalization results and compared to the exact data at extreme points. Numerical analysis shows that the ground state is non-degenerate ($S_T^z = 0$), while the first excited state is doubly degenerate ($S_T^z = \pm 1$) for both the cases and throughout the regime $0 \leqslant \Delta < 1$. Although the ground state remains unique, spin gap is found to develop in the excitation spectrum as soon as the non-uniformity is introduced in AFM-AFM chain. The spin gap remains non-zero in most of the AFM-FM region. The non-uniformity of bond strengths in a bond alternating system breaks the full translational symmetry of the model. The gap attributes to the breaking of this translational symmetry which ultimately gives rise to the Haldane phase. Spin gap, string orders and dimer order have been obtained numerically. Spin gap and string orders are found to coexist and non-zero throughout the parameter regime apart from the point $J_2/J_1 = -1$, $\Delta = 0$ and line $J_2/J_1 = 1$, $0 < \Delta < 1$. This phenomenon attributes to the existence of Haldane phase. Thus, the Haldane phase is present in the whole parameter regime apart from the point $J_2/J_1 = -1$, $\Delta = 0$ and line $J_2/J_1 = 1$, $0 \leqslant \Delta \leqslant 1$, like the existence of the same at the isotropic point, $J_2/J_1 \neq 1$, $\Delta = 1$. In other words, the Haldane phase is not only present at the isotropic point but in most of the anisotropic regime of the bond alternating spin-1/2 Heisenberg chain. However, the nature of decay of the parameters E_{Gap}, O_D, O_S^z and O_S^x indicates that they all will vanish at larger values of $|J_2/J_1|$ beyond $J_2/J_1 = -1$ in FM J_2 region for $0 < \Delta \leqslant 1$, which hints at the collapse of Haldane phase. For this case, it is expected that either Néel or chiral ordered phase may appear in that region by replacing the Haldane phase.

7.1. Acknowledgements

References

1. Griffiths R.B., Phys. Rev., 1964, **133**, A768, doi:10.1103/PhysRev.133.A768.
2. Haldane F.D.M., Phys. Rev. Lett., 1983, **50**, 1153, doi:10.1103/PhysRevLett.50.1153.
3. Den Nijs M., Rommelse K., Phys. Rev. B, 1989, **40**, 4709, doi:10.1103/PhysRevB.40.4709.
4. Tasaki H., Phys. Rev. Lett., 1991, **66**, 798, doi:10.1103/PhysRevLett.66.798.
5. Lieb E., Schultz T., Mattis D., Ann. Phys., 1961, **16**, 407, doi:10.1016/0003-4916(61)90115-4.
6. Affleck I., Lieb E.H., Lett. Math. Phys., 1986, **12**, 57, doi:10.1007/BF00400304.
7. Hastings M.B., Phys. Rev. B, 2004, **69**, 104431, doi:10.1103/PhysRevB.69.104431.
8. Bulaevskii L.N., Sov. Phys. JETP, 1963, **17**, 684.
9. Brooks Harris A., Phys. Rev. B, 1973, **7**, 3166, doi:10.1103/PhysRevB.7.3166.
10. Southern B.W., Martínez Cuéllar J.L., Lavis D.A., Phys. Rev. B, 1998, **58**, 9156, doi:10.1103/PhysRevB.58.9156.
11. Kohmoto M., Tasaki H., Phys. Rev. B, 1992, **46**, 3486, doi:10.1103/PhysRevB.46.3486.
12. Totsuka K., Phys. Lett. A, 1997, **228**, 103, doi:10.1016/S0375-9601(97)00087-X.
13. Affleck I., Kennedy T., Lieb E.H., Tasaki H., Phys. Rev. Lett., 1987, **59**, 799, doi:10.1103/PhysRevLett.59.799.
14. Affleck I., Kennedy T., Lieb E.H., Tasaki H., Commun. Math. Phys., 1988, **115**, 477, doi:10.1007/BF01218021.
15. Hida K., Phys. Rev. B, 1992, **45**, 2207, doi:10.1103/PhysRevB.45.2207.
16. Sakai T., J. Phys. Soc. Jpn., 1995, **64**, 251, doi:10.1143/JPSJ.64.251.
17. Hase M., Terasaki I., Uchinokura K., Phys. Rev. Lett., 1993, **70**, 3651, doi:10.1103/PhysRevLett.70.3651.
18. Jacobs I.S., Bray J.W., Hart H.R. (Jr.), Interrante L.V., Kasper J.S., Watkins G.D., Prober D.E., Bonner J.C., Phys. Rev. B, 1976, **14**, 3036, doi:10.1103/PhysRevB.14.3036.
19. Cross M.C., Fisher D.S., Phys. Rev. B, 1979, **19**, 402, doi:10.1103/PhysRevB.19.402.
20. Huizinga S., Kommandeur J., Sawatzky G.A., Thole B.T., Kopinga K., de Jonge W.J.M., Roos J., Phys. Rev. B, 1979, **19**, 4723, doi:10.1103/PhysRevB.19.4723.
21. Yamaguchi H., Shinpuku Y., Shimokawa T., Iwase K., Ono T., Kono Y., Kittaka S., Sakakibara T., Hosokoshi Y., Preprint arXiv:1502.06804v1, 2015.
22. Watanabe S., Yokoyama H., J. Phys. Soc. Jpn., 1999, **68**, 2073, doi:10.1143/JPSJ.68.2073.
23. Kodama K., Harashina H., Sasaki H., Kato M., Sato M., Kakurai K., Nishi M., J. Phys. Soc. Jpn., 1999, **68**, 237, doi:10.1143/JPSJ.68.237.

24. Miura Y., Hirai R., Kobayashi Y., Sato M., J. Phys. Soc. Jpn., 2006, **75**, 084707, doi:10.1143/JPSJ.75.084707.
25. Manaka H., Yamada I., Honda Z., Katori H.A., Katsumata K., J. Phys. Soc. Jpn., 1998, **67**, 3913, doi:10.1143/JPSJ.67.3913.
26. Stone M.B., Tian W., Lumsden M.D., Granroth G.E., Mandrus D., Chung J.-H., Harrison N., Nagler S.E., Phys. Rev. Lett., 2007, **99**, 087204, doi:10.1103/PhysRevLett.99.087204.
27. White S.R., Affleck I., Phys. Rev. B, 1996, **54**, 9862, doi:10.1103/PhysRevB.54.9862.
28. Sachdev S., Bhatt R.N., Phys. Rev. B, 1990, **41**, 9323, doi:10.1103/PhysRevB.41.9323.
29. Jordan P., Wigner E., Z. Phys., 1928, **47**, 631, doi:10.1007/BF01331938.
30. Verkholyak T., Honecker A., Brenig W., Eur. Phys. J. B, 2006, **49**, 283, doi:10.1140/epjb/e2006-00077-1.
31. Wang Y.R., Phys. Rev. B, 1992, **46**, 151, doi:10.1103/PhysRevB.46.151.
32. Grosso G., Martinelli L., Parravicini G.P., Phys. Rev. B, 1995, **51**, 13033, doi:10.1103/PhysRevB.51.13033.
33. Broeck J.-M.V., Schwartz L.W., SIAM J. Math. Anal., 1979, **10**, 658, doi:10.1137/0510061.
34. Bulirsch R., Stoer J., Numer. Math., 1964, **6**, 413, doi:10.1007/BF01386092.
35. Hida K., J. Phys. Soc. Jpn., 1993, **62**, 1463, doi:10.1143/JPSJ.62.1463.
36. Hida K., Phys. Rev. B, 1992, **46**, 8268, doi:10.1103/PhysRevB.46.8268.

Властивості основного стану спін-$\frac{1}{2}$ анізотропного гайзенбергівського ланцюжка з перемінними зв'язками

С. Пол[1], А.К. Гош[2]

[1] Фізичний факультет, Шотландський церковний коледж, Колката 700006, Індія

[2] Фізичний факультет, Джадавпурський університет, Колката 700032, Індія

Досліджено властивості основного стану, дисперсійні співвідношення і скейлінгову поведінку спінової щілини спін-$\frac{1}{2}$ анізотропного гайзенбергівського ланцюжка з перемінними зв'язками, коли обмінна взаємодія на навперемінних зв'язках є феромагнітною (FM) і антиферомагнітною (AFM) в двох окремих випадках. Результуючі моделі порізно представляють ланцюжки з сусідніми (NN) AFM-AFM і AFM-FM навперемінними зв'язками. Енергію основного стану оцінено аналітично за допомогою представлення оператора зв'язку так і представлення Джордана-Вігнера, а також чисельно, використовуючи точну діагоналізацію. Отримано дисперсійні співвідношення, спінову щілину і декілька типів впорядкування основного стану. Знайдено, що димерне впорядкування і стрічкові впорядкування співіснують в основному стані. Знайдено, що спінова щілина появляється як тільки вводиться неоднорідність сили навперемінних зв'язків в AFM-AFM ланцюжку, яка далі залишається ненульовою для AFM-FM ланцюжка. Ця спінова щілина вздовж стрічкових впорядкувань є характерною ознакою фази Галдейна. Знайдено, що фаза Галдейна існує в більшості анізотропної області подібно до ізотропної точки.

Ключові слова: *навперемінні зв'язки, спінова щілина, оператор зв'язку, стрічкові впорядкування, димерне впорядкування, скейлінговий закон*